GCA
CORPORATION
Bedford, Massachusetts

[redacted]

Prepared for

NATIONAL AERONAUTICS AND SPACE ADMINISTRATION
Headquarters
Washington, D. C. 20546

by

Dr. F. F. Marmo, Project Director and
Principal Investigator

July 1965

EXPERIMENTAL AND THEORETICAL STUDIES IN PLANETARY AERONOMY

Quarterly Progress Report

Covering the Period 18 March 1965
through 30 June 1965

Prepared under Contract No. NASW-1283

TABLE OF CONTENTS

I. INTRODUCTION

This is the First Quarterly Progress Report which describes the technical progress from 5 April 1965 through 5 July 1965 under NASA Contract No. NASW-1283. Scientific investigations accomplished during the current reporting period resulted in the generation of the following papers submitted and/or accepted for publication in accredited scientific journals, books and/or GCA Technical Reports or presented at scientific meetings.

Technical Papers Submitted and/or Accepted for Publication

	Publication
a. Submitted	
The Total Absorption Cross Sections of H_2, N_2 and O_2 in the Region 550 to 200Å (J.A.R. Samson and R. B. Cairns)	J. Opt. Soc. Am.
The Measurement of the Photoionization Cross Sections of the Atomic Gases (J.A.R. Samson)	Atomic & Molecular Processes, ed. D.Bates (Academic Press, in press)
The Fluorescence of Solar Ionizing Radiation (A. Dalgarno and M. B. McElroy)	Planetary Space Sci.; GCA TR No. 65-15-N
b. Accepted	
The Refractive Index of Helium (Rayleigh Scattering by Helium) (Y. M. Chan and A. Dalgarno)	Proc. Phys. Soc. 85, 227 (1965); GCA TR No. 65-14-N

Published GCA Technical Reports

	GCA TR No.
PHYSICS OF PLANETARY ATMOSPHERES I: Rayleigh Scattering by Helium (Y. M. Chan and A. Dalgarno)	65-14-N (April 1965)
PHYSICS OF PLANETARY ATMOSPHERES II: The Fluorescence of Solar Ionizing Radiation (A. Dalgarno and M.B.McElroy)	65-15-N (May 1965)

Technical Papers Presented at Scientific or Professional Meetings

Photoionization Processes (J.A.R. Samson) – INVITED PAPER presented by J.A.R. Samson at Thirteenth Annual Conference on Mass Spectroscopy and Allied Topics, St. Louis, Missouri, on May 17-18, 1965.

Oscillator Strengths in the Noble Gases (J.A.R. Samson) – INVITED PAPER presented by J.A.R. Samson at the Thirteenth Annual Meeting of the Radiation Research Society in Philadelphia, Pa., on May 25-26, 1965.

In Section II, technical summaries are given on the work performed under the present contract. During the current reporting period, significant progress has been achieved in three areas:

A. Theoretical studies,

B. Experimental investigations in the VUV and EUV spectral regions

and finally,

C. Planetary aeronomy.

Accordingly, the progress is discussed in that order.

In Section III, miscellaneous items are reported which are considered to be pertinent to the performance of the contract requirements. These items include the description of additional work performed which represent logical extension of efforts under the present investigations. In addition, this section reports miscellaneous information on the attendance and presentation of papers at scientific meetings with brief descriptions of technical papers considered to be important to the efficient performance of the present study program.

II. TECHNICAL SUMMARIES OF WORK PERFORMED UNDER THE PRESENT CONTRACT

The technical progress accomplished during the current reporting period can be conveniently discussed in three categories:

A. Theoretical studies,

B. Experimental investigations in the VUV and EUV spectral regions, and

C. Planetary aeronomy.

A. THEORETICAL STUDIES

Progress under theoretical studies has resulted in the generation of two reports which have been submitted and/or accepted for publication. Two important areas were investigated. First, accurate values for Rayleigh scattering by helium have been computed so that these could be incorporated with the measured scattering cross section previously reported under the present program.[1] The theoretical techniques are being extended to apply to more complex atoms; a cross check will again be available when these new values are compared to experimental values cited above.

The second area of investigation was concerned with the determination of the fluorescence of O^+, N_2^+ and O_2^+ due to solar photoionization. The study has shown that it is possible to continuously probe the ionosphere and the ultraviolet solar activity by either earth-bound or rocket-borne optical experimentation. This important finding affords a new dimension in optical experimental probing of the earth's atmosphere. Technical summaries of these investigations are given below.

1. Rayleigh Scattering by Helium

The cross section for the scattering of light by an atomic gas may be obtained from the refractive index.

The refractive index of helium has been measured with high precision at wavelengths between 2700 and 5400Å[2] and the measurements can be extrapolated to longer wavelengths without serious loss of accuracy. The extrapolation to shorter wavelengths has been carried out using a semi-empirical procedure,[3] but the accuracy is uncertain. The refractive index can be calculated directly at any wavelength by variational procedures similar to those employed in the calculation of static polarizabilities and with comparable accuracy.

Our procedure, which relates the evaluation of infinite summations to the solutions of differential equations, differs in its approach from those discussed by Karplus et al.[4-8]

The refractive index n of a gas of number density N is given by

$$n - 1 = 2\pi N\alpha(\nu) \tag{1}$$

where $\alpha(\nu)$ is the frequency-dependent atomic or molecular polarizability. If the atom or molecule is in a state with eigenfunction ψ_0 and ψ_s represents the eigenfunctions of the other quantum states

$$\alpha(\nu) = \frac{2}{3h} \sum{}' \frac{\nu_{s0}}{\nu_{s0}^2 - \nu^2} |(0|\underline{m}|s)|^2 \tag{2}$$

where ν_{s0} is the eigenfrequency of the transition from ψ_0 to ψ_s and $\underline{m}$ is the electric dipole moment

$$\underline{m} = \sum_i e_i \underline{r}_i \tag{3}$$

e_i being the charge of the i<u>th</u> particle and $\underline{r}_i$ being its position vector. The polarizability (Eq. 2) can be written alternatively as

$$n - 1 = \frac{1}{3h} \sum_s{}' \left(\frac{1}{\nu_{s0}+\nu} + \frac{1}{\nu_{s0}-\nu} \right) |(0|\underline{m}|s)|^2 \tag{4}$$

or as

$$n - 1 = \frac{1}{12\pi^2 m\nu^3} \sum_s{}' \left(\frac{1}{\nu_{s0}+\nu} - \frac{1}{\nu_{s0}-\nu} \right) (0|\underline{m}|s)(s|\underline{m}'|0) \tag{5}$$

where $\underline{m}'$ is the electric gradient operator

$$\underline{m}' = \sum_i e_i \nabla_i \ . \tag{6}$$

Now introducing a function $\chi(\underline{r}_i/\nu)$ such that

$$(H - E_0 + h\nu)\ \chi(\nu) + \underline{m}\psi_0 = 0 \tag{7}$$

where

$$(H - E_0)\ \psi_0 = 0 \ , \tag{8}$$

it may be shown (cf. Dalgarno, Refs. 9, 10) that Eq. (4) is equivalent to

$$n - 1 = \frac{1}{3}[\{\chi(\nu) + \chi(-\nu)\},\ \underline{m}\psi_0] \tag{9}$$

and Eq. (5) to

$$n - 1 = \frac{h}{12\pi^2 m\nu^3} [\{\chi(\nu) - \chi(-\nu)\},\ \underline{m}'\psi_0] \ . \tag{10}$$

Equation (10) can be written alternatively as

$$n - 1 = \frac{h}{12\pi^2 m\nu^3} [\{\chi'(\nu) - \chi'(-\nu)\}, \underline{m}\psi_0] \tag{11}$$

where

$$(H - E_0 + h\nu)\chi'(\nu) + \underline{m}'\psi_0 = 0 \ . \tag{12}$$

Equation (7) may be solved by constructing a functional

$$J(\nu) = \{\chi(\nu)|H - E_0 + h\nu|\chi(\nu)\} + 2\{\chi(\nu), \underline{m}\psi_0\} \tag{13}$$

and minimizing $J(\nu)$ with respect to some trial form of $\chi(\nu)$. Then

$$\alpha(\nu) = \tfrac{1}{3}\{J(\nu) + J(-\nu)\} \tag{14}$$

is a lower bound to the polarizability (provided ψ_0 is an exact eigenfunction of H).

We adopted for the ground state of helium the 20-parameter representation of Hart and Herzberg[11] and a trial function $\chi t(\nu)$ of the form

$$\chi t(\nu) = \sum_{s=0}^{m} c_s(\nu)(\underline{r}_1 r_1{}^s + \underline{r}_2 r_2{}^s)\psi_0(\underline{r}_1, \underline{r}_2) \tag{15}$$

the $c_s(\nu)$ being variational parameters. Substituted into Eq. (14) they yield a static polarizability ($\nu = 0$) of 0.204×10^{-24} cm^3 in close agreement with the most accurate value available: 0.205×10^{-24} cm^3.[12]

As Table 1 demonstrates, the convergence of $\alpha(\nu)$ as a function of the number of variational parameters is very rapid for the visible region of the spectrum but less so as the first resonance wavelength is approached. The

TABLE 1

Convergence of $\alpha(\nu)$

Wavelength (Å) \ m	0	1	2	3	4
9110	1.132	1.378	1.379	1.379	- 1.379
3037	1.147	1.413	1.414	1.414	1.414
911	1.319	1.905	1.950	1.952	1.952
759	1.422	2.307	2.452	2.465	2.467
607	1.661	3.869	5.507	6.342	6.786
569	1.775	5.288	13.18	56.86	- 38.61

proper change in the sign of $J(\nu)$ does occur as the wavelength is decreased, the first pole occurring at 573Å compared with the correct location of 584Å. Attempts to proceed to larger numbers of variational parameters led to serious numerical instabilities.

The values of n - 1 measured by Cuthbertson and Cuthbertson,[2] which refer to wavelengths longer than 2750Å, exceed the predicted values by 0.44 percent near 9000Å, the excess increasing to 0.50 percent at 2750Å. We have accordingly increased the theoretical values uniformly by 0.47 percent and they are presented in Figures 1 and 2, which include also the measured values.

The cross section for the scattering of isotropic, unpolarized radiation is given by

$$Q = \frac{128\pi^5}{3\lambda^4}\,\alpha(\nu)^2 \tag{16}$$

and values of Q may be readily derived from Figures 1 and 2.

The cross section for scattering of Lyman-α is 3.53×10^{-26} cm^2. Values for some other wavelengths are given in Table 2.

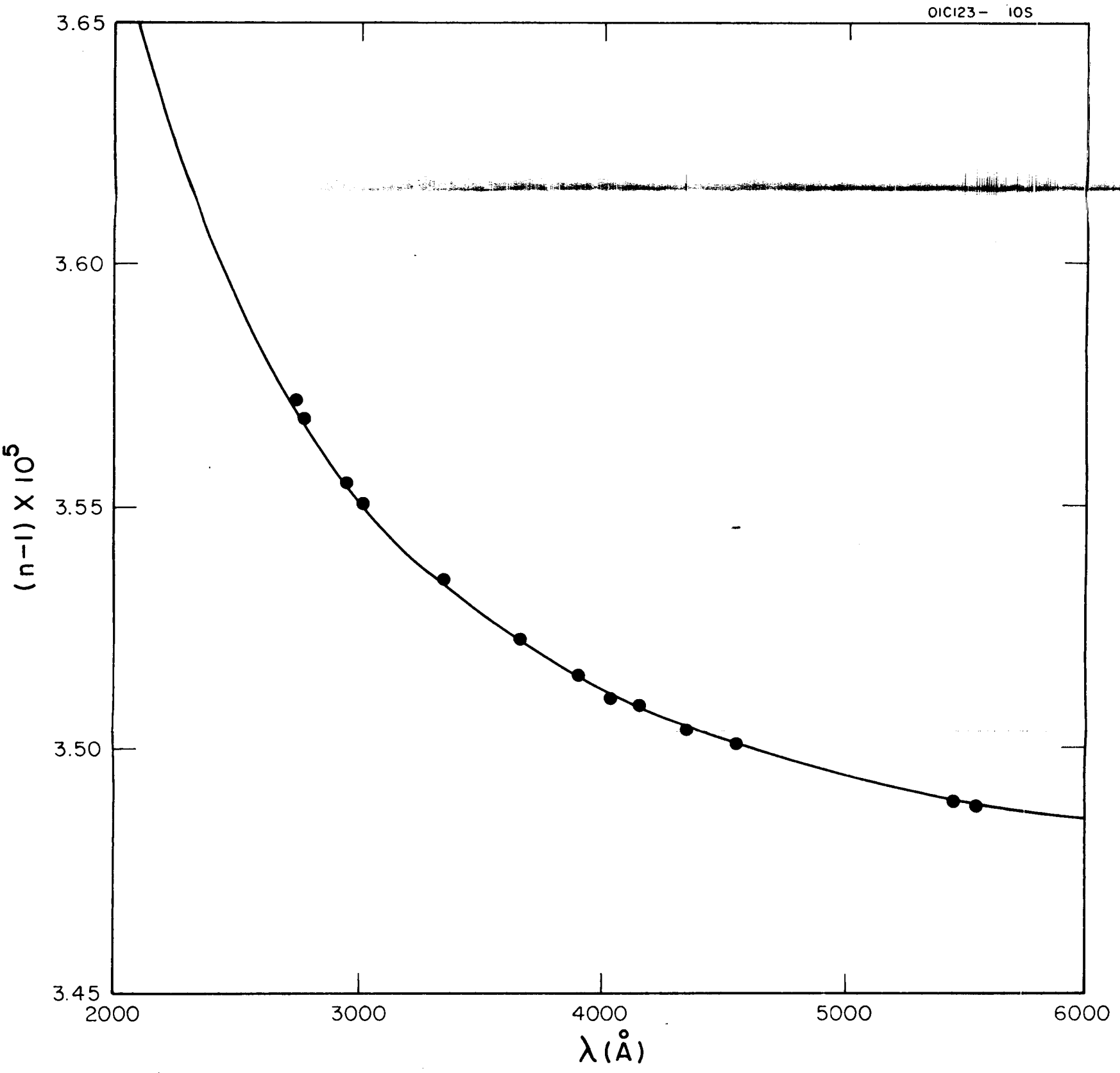

Figure 1. The refractive index of helium.

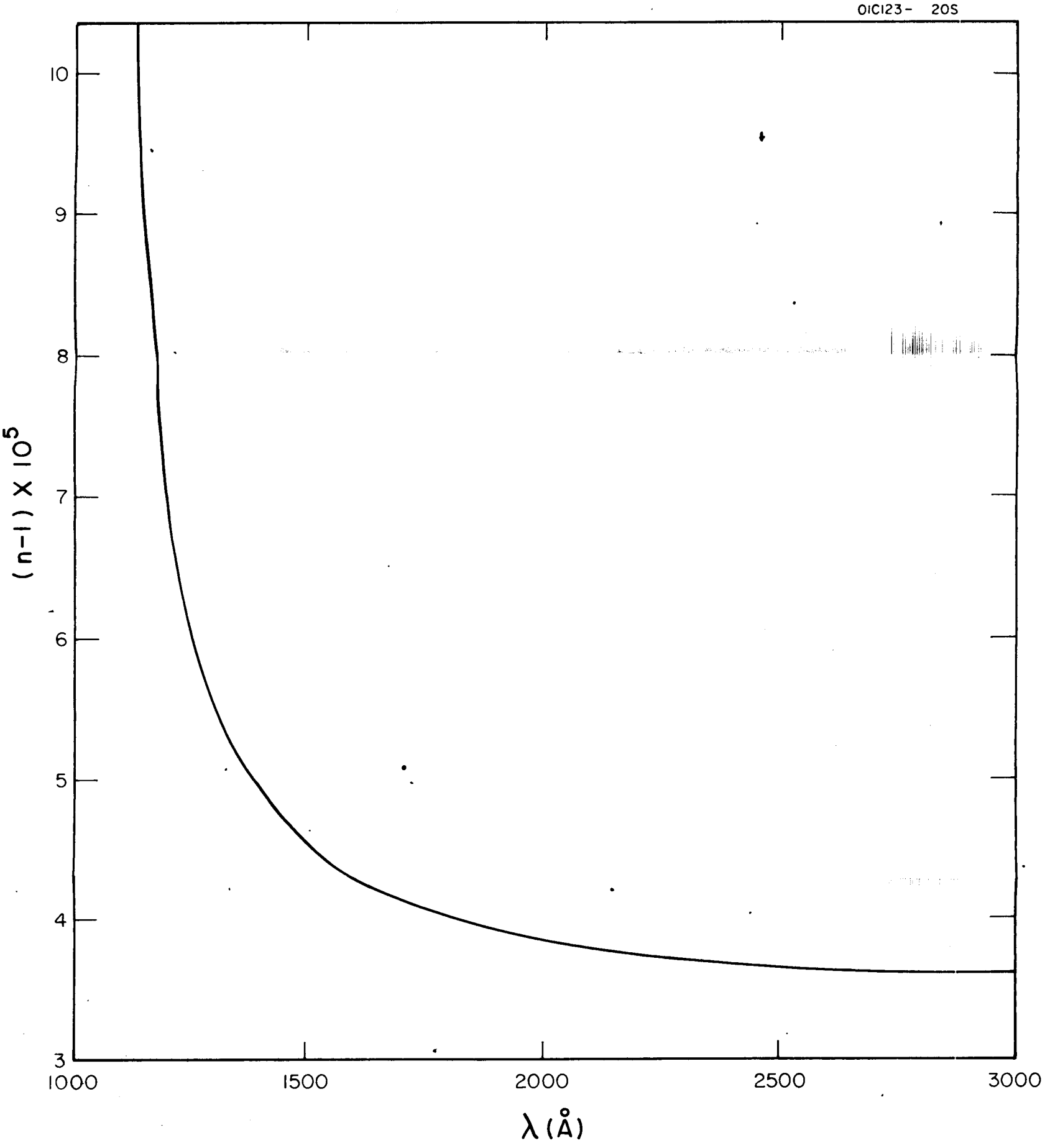

Figure 2. The refractive index of helium.

TABLE 2

Light Scattering Cross Sections Q cm^2

(Å)	700	800	1000	1500	2000	2500
$Q(cm^2)$	1.07×10^{-24}	3.56×10^{-25}	9.51×10^{-26}	1.33×10^{-26}	3.83×10^{-27}	1.50×10^{-27}

2. The Fluorescence of Solar Ionizing Radiation

When solar ultraviolet radiation ionizes an atmospheric constituent the positive ion may be left in an excited electronic level which can then radiate. In this study the atmospheric constituents considered are those of atomic oxygen, molecular oxygen and molecular nitrogen. It will be shown that the resulting fluorescent emission may be detectable in rocket-borne (ultraviolet and visible) or ground-level instrumentation, thereby providing an optical method for the investigation of ionospheric behavior. In particular, the study shows that it should be possible to monitor the solar ultraviolet ionizing radiations by performing experiments in the visible regions on O^+ radiations. Only minimum details are given in the summary report since they are available in publication form. However, a brief, self-contained discussion on the technique employed is given below.

Concerning the ion production rates, the original report gives a rather detailed account of all the possibilities due to the photoionizing of atomic oxygen, molecular oxygen and molecular nitrogen. For example, it is shown that for the case of atomic oxygen, spectral heads are located at 910Å, 732Å, 663Å, 434Å and 310Å. Corresponding cases for molecular nitrogen are 796Å, 732Å, 661Å and 350Å. For molecular oxygen, emissions can be expected at 1026Å, 767Å, 729Å and 682Å. Obviously, each of these cases depends upon what excitation mechanism is assumed. They are not specifically enumerated here. The appropriate photoionization cross sections were employed as follows. For the case of atomic oxygen, the theoretical values calculated in an earlier study under the present program[13] were employed. It may be recalled that in

this study, the required individual transitions were investigated. In fact, this was one of the important purposes for performing that study. The appropriate cross sections for molecular nitrogen and oxygen for individual transitions are not as well known. For this reason, it was assumed that whenever the photon energy is such that a multiplicity of ionizing transitions can occur, the probability of a particular transition is then proportional to the statistical weight of the produced positive ion states. For the ground-state molecules, the measured total cross sections due to Huffman, Tanaka and Larrabee,[14] Cook, Ching and Becker,[15] and Samson and Cairns[16] were used. Schoen[17] recently gave estimates of the percentages of photoionizing transitions in molecular oxygen and nitrogen which terminate in particular states. These considerations were also incorporated into the present theoretical study.

Processes which remove excitation in the excited ions were discussed in detail in the original paper and are not repeated here. However, suffice it to say that excited ions of the three species O^+, O_2^+ and N_2^+ were considered. Thus, the exciting and decay mechanisms were then integrated into a consistent theoretical approach to produce the data shown in Figures 3 through 7. As stated previously, the figures make evident that the predicted fluorescence signal levels are compatible to observations by conventional rocket-borne or earth-bound instrumentation. The value of this important new tool for continuous monitoring of ionospheric behavior and solar ultraviolet activity cannot be overemphasized at this point.

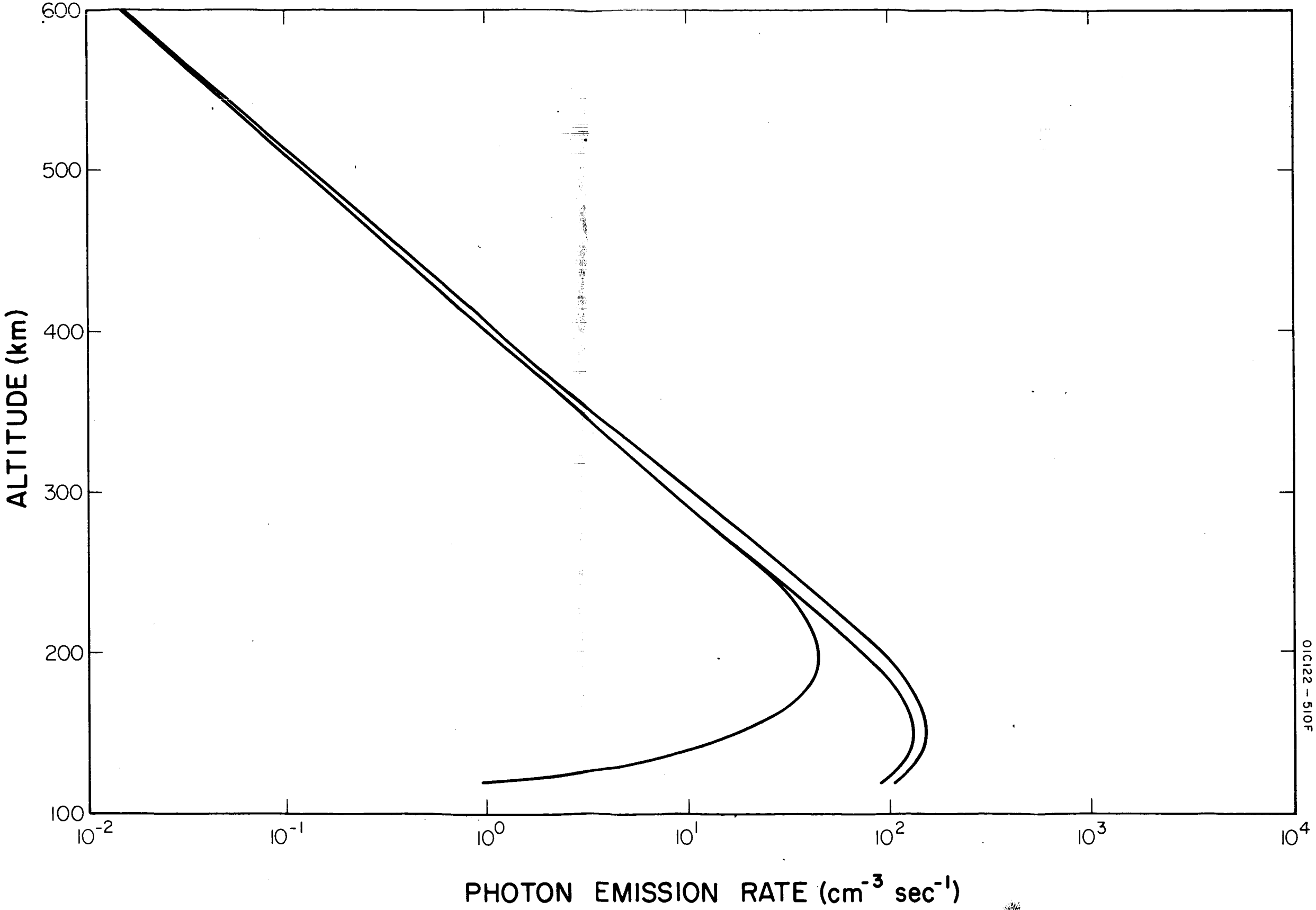

Figure 3. The altitude profile of fluorescent emission at noon from the $O^{+}(^{2}P - ^{2}D)$ transition. From right to left, the curves show the inclusion of electron impact deactivation and molecular nitrogen impact deactivation.

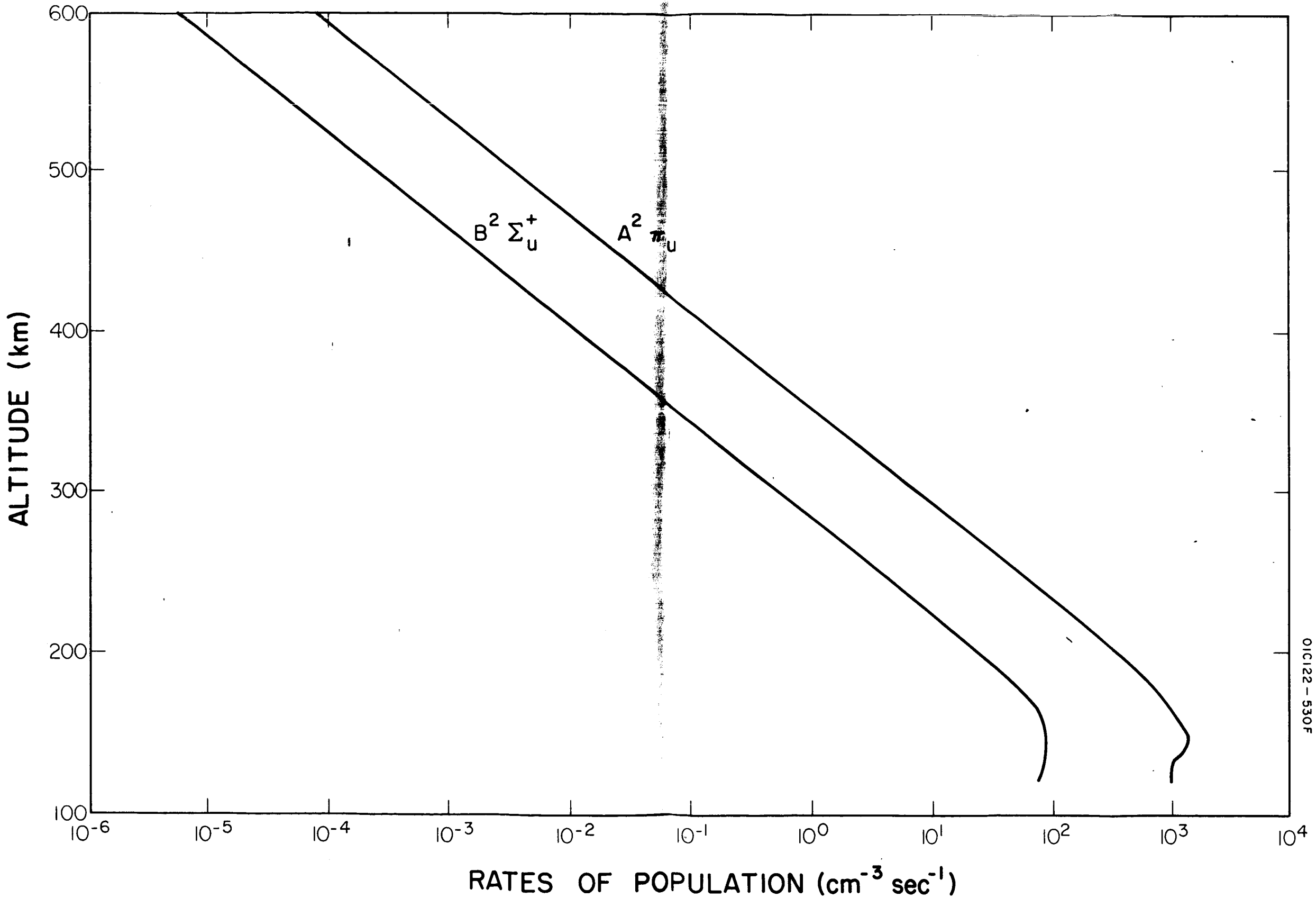

Figure 4. The rates of population at noon of the upper levels $A^2 \pi_u$ and $B^2 \Sigma_u^+$ of respectively the Meinel and the first negative band systems of nitrogen.

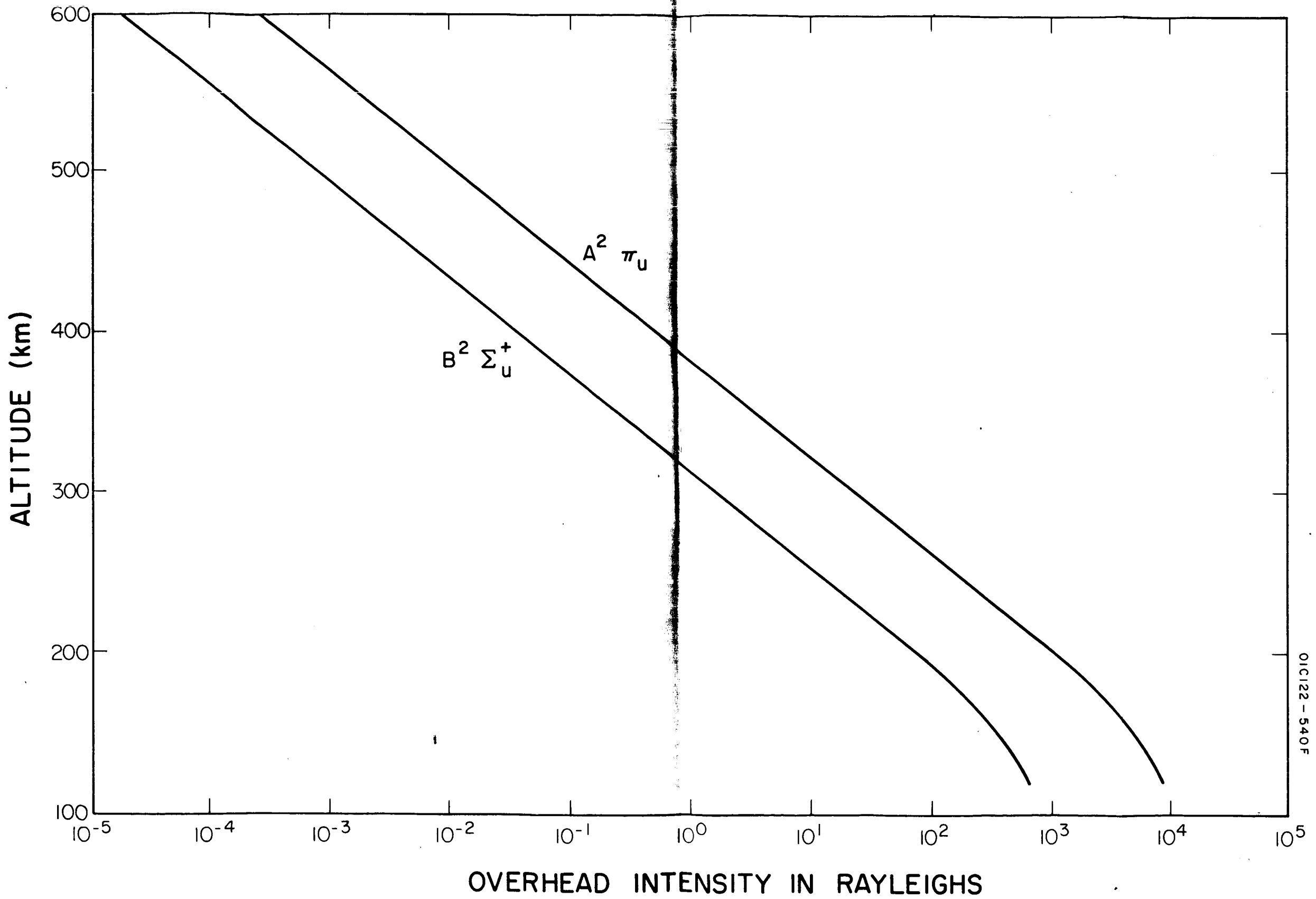

Figure 5. The overhead intensities of the Meinel and first negative band systems of nitrogen.

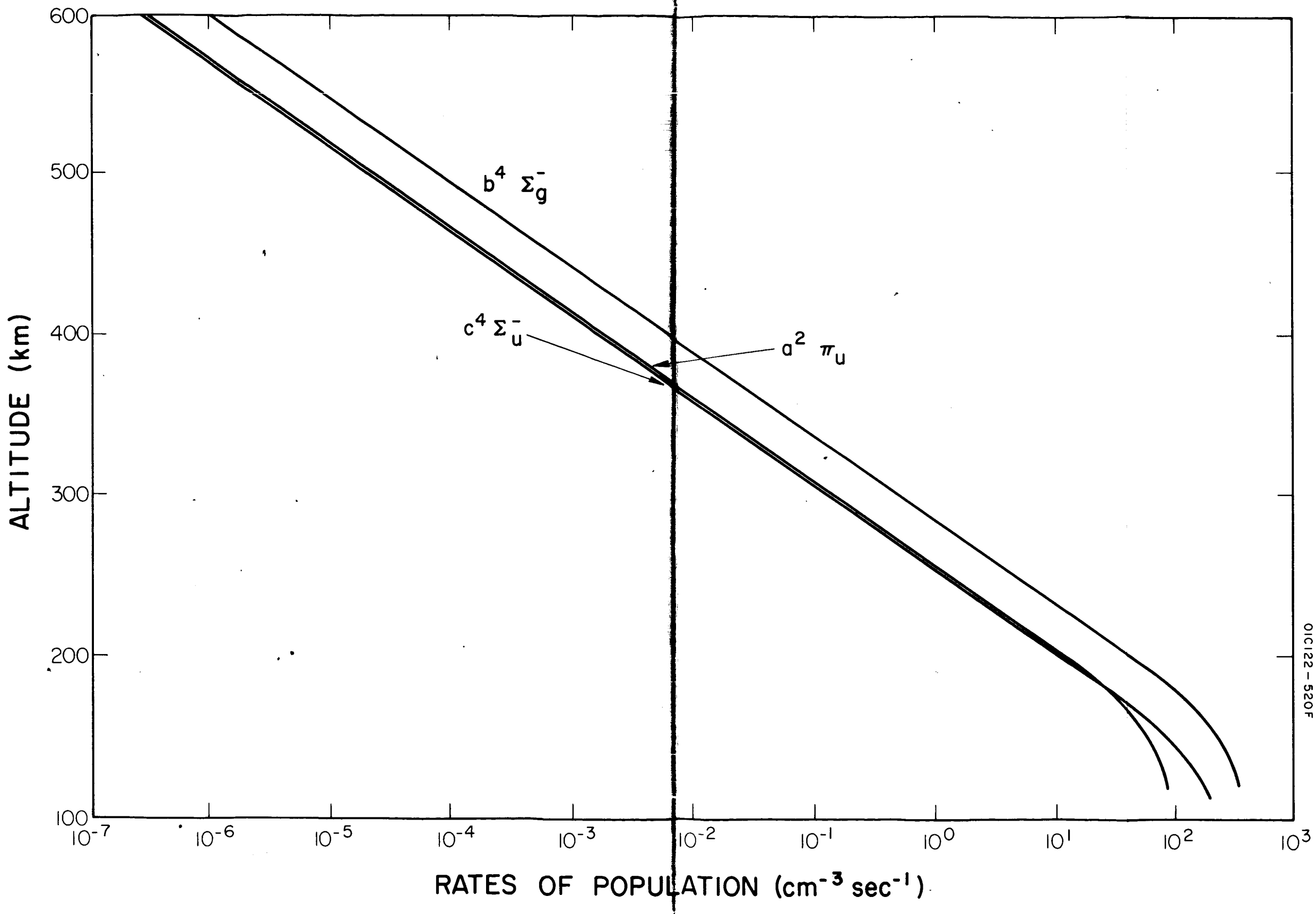

Figure 6. The rate of population at noon of the upper levels $C^4\ \Sigma_u^-$, $b^4\Sigma_g^-$ and $a^2\pi_u$ of respectively, the Hopfield and the first and second negative band systems of oxygen.

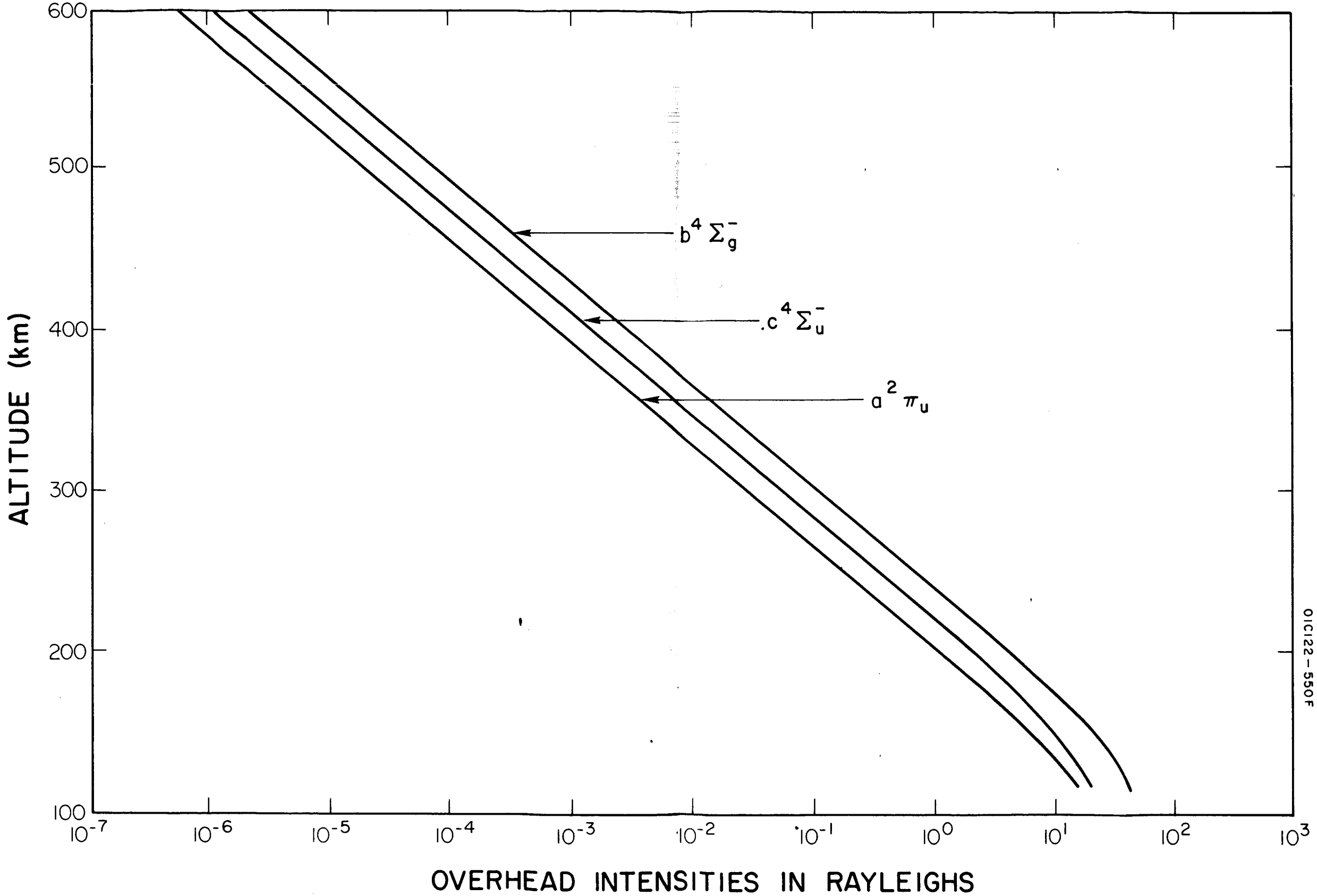

Figure 7. From right to left the curves show the overhead intensities of the first negative, the Hopfield and the second negative systems of oxygen.

B. EXPERIMENTAL INVESTIGATIONS IN THE VUV AND EUV SPECTRAL REGIONS

During this Quarter, effort has been directed toward three scientific areas:

1. the determination of the total absorption cross sections of H_2, N_2 and O_2 in the region 550 to 200Å,

2. determination of electron energies due to the photoionization of planetary gases, and

3. studies on the ionization potential of O_2 as a function of temperature.

1. Total Absorption Cross Sections of H_2, N_2 and O_2 in the Region 550 to 200Å.

Owing to the ready availability of the pertinent experimental apparatus, it was decided to extend absorption cross-section measurements for H_2, N_2 and O_2 into the short wavelength region of 550 to 200Å. The results of this work have been submitted to the Journal of the Optical Society of America for publication in a future issue. A brief technical summary is given below.

Values of the total absorption cross sections of H_2, N_2 and O_2 measured at wavelengths between 550 and 200Å are listed in Table 3. The experimental techniques employed have been previously described.[16] The data have an estimated accuracy of ± 10 percent. The measured cross sections of the three gases were not pressure dependent and decreased monotonically

TABLE 3

ABSORPTION CROSS SECTIONS OF H_2, N_2 AND O_2

Wavelength (Å)	Absorption Cross Section (10^{-18} cm^2)		
	H_2	O_2	N_2
209.3	0.266	9.04	6.46
225.2		10.6	
234.2	0.402	10.6	
239.6	0.439	11.9	
247.2	0.494	12.3	9.75
260.5	0.579		
266.3	0.638	14.0	10.5
283.5	0.790	15.2	10.9
297.6	0.949		11.5
303.1	1.02	16.3	11.6
314.9	1.12	16.4	12.4
323.6	1.22	16.7	13.1
335.1	1.36	16.8	14.0
345.1	1.51	17.0	14.8
358.5	1.75		15.7
362.9	1.84	17.5	16.1
374.4	2.04	17.9	17.3
387.4	2.26	18.5	18.6
428.2	2.88	19.4	22.1
434.3	3.02	19.6	22.4
452.2	3.37		22.6
463.7			22.6
508.2		23.7	22.8
512.1			23.2
519.6		25.2	25.8
522.2		20.9	23.6
525.8		24.5	26.2
537.0		21.2	25.2

from 500Å to shorter wavelengths. It is, therefore, probable that they delineate the absorption continua appropriate to this region. There is no agreement with the results previously reported for O_2[16,18-21] and N_2[16,22-24] with the exception of those of Po Lee[21] and Samson and Cairns.[16]

2. Electron Energies Due to the Photoionization of Planetary Gases

In this experimental area it is critical to develop a suitable electron analyzer. An early model has been previously described.[25] It has been shown that with this prototype analyzer coupled to a VUV monochromator, one is able to measure at least the gross features of the resulting electron energy spectrum due to the photoionization of A, N_2 and O_2. However, for quantitative results, it is mandatory that the analyzer must display a higher resolving power in terms of electron energy discrimination. During this Quarter, a considerable effort in the redesign of the prototype has been achieved. As a result of these investigations, two modifications have been indicated. First, the inner cylindrical mesh is now being replaced by a system of disks in order to select only those electrons which travel at right angles to the incident radiation. Second, the total length of the analyzer is being increased so that it will be possible to preserve the cm^2-column count and to use a lower gas pressure in order to avoid excessive scattering of the electrons. The optimum spacing and number of disks and analyzer length are presently being determined on the basis of actual laboratory runs.

3. Ionization Potential of O_2

The first ionization potential of any gas can in principle be obtained from a detailed analysis of its absorption spectrum. Such an analysis involves the identification of a Rydberg-type series, the limit of which corresponds to the ionization potential of the gas. Other major techniques used for the determination of ionization potentials are (a) the cyclic method, using known dissociation energies, (b) electron impact methods, and (c) photon impact methods. The most precise method is that of a Rydberg analysis. In oxygen, however, the spectrum in the region close to threshold is so complicated that as yet no Rydberg series has been identified leading to the first ionization potential. Methods (a), (b) and (c) have provided the ionization potential of O_2 with values ranging from 12.5 to 12.04 eV. Of these, (c) is employed in the present work. It is desirable to know the ionization threshold more accurately for in addition to its fundamental importance in molecular spectroscopy, its precise value is important to ionospheric physics since some important solar emission lines lie within this energy range.

The photoionization onset potential of O_2 was first studied by Inn[26] who observed ions at wavelengths as long as 1029Å. Watanabe and Marmo[27] also reported ions in this region. They measured the photoionization yield at 1030.8Å and found a value of 0.7 percent whereas at 1025.7Å, the yield was found to be 58 percent. Watanabe and Marmo ascribed the low yield at 1030.8Å as being due to the photoionization of those molecules which are

normally in vibrationally-excited states at room temperature. With this interpretation, they define the break in the ionization yield curve at 1026.5 ± 1Å (12.08 ± .01 eV) as the ionization potential of O_2. Although the ionization potential is lowered at room temperature for molecules initially in higher vibrational states, only 0.6 percent of the molecules are in the first vibrational state and a negligible number in higher vibrational states. The photoionization curve might, therefore, be expected to have a single small step approximately 20Å long (one vibrational spacing) preceding the sharp rise at the true ionization potential. However, Watanabe and Marmo observed ions only 4Å beyond their quoted onset potential. This can probably be explained by the fact that the radiation was not totally absorbed in their ion chamber for this wavelength region and, therefore, the ion currents would be too small to be measured. Their maximum gas pressure was 2 torr and the length of the parallel plate electrodes was 11 cm. For total absorption of the radiation at 1030Å, a pressure of approximately 20 torr would be necessary. Nicholson[28] studied the photoionization cross section of oxygen at considerably lower pressures (~ 100 μ). He obtained only the relative cross sections since he used the low pressure approximation that the ratio of the measured ion currents to the incident photon intensity is proportional to the photoionization cross section. He obtained an onset potential of 1027.57 ± 0.26Å (12.065 ± 0.003 eV). Thus, the question can be raised as to whether molecules in vibrational states are involved in the ionization process.

With the present experimental setup, the ion currents produced by the photoionization of oxygen were measured under conditions of maximum sensitivity and were found to have an appearance potential of 1046.4 ± 1Å (11.85 ± 0.01 eV). The photoionization cross sections ($\sigma_i = \gamma\sigma$) were measured from 900 to 1050Å. The results are shown in Fig. 8. Before describing the figure in detail, it is important to establish the reality and nature of the ion currents observed at wavelengths longer than the presently-accepted ionization potential of 1026.5Å. In a separate experiment, using a mass spectrometer coupled to a vacuum monochromator, the ions were observed to be O_2^+ ions at least for wavelengths as long as 1030Å. The sensitivity of the mass spectrometer was insufficient to observe the small ion currents formed at longer wavelengths.

As can be seen from Fig. 8, σ_i increases rapidly between 1030 and 1026.5Å. Since the wavelength resolution is 0.9Å, this increase is real and not instrumental. This increase cannot be accounted for on the basis of ionization of molecules in rotationally excited states due to the selection rules. As far as ionization of vibrationally-excited molecules is concerned, the observed ion currents appear to be much too large.

A conclusive test of the possibility of ionization from excited vibrational levels would be to cool the gas. At dry ice temperature (- 80°C), the population of the first vibrational level is reduced by a factor of 10 and at liquid oxygen temperature (- 188°C), the reduction would be a factor of 10^9 from that at room temperature. Thus, a correspondingly large decrease in the

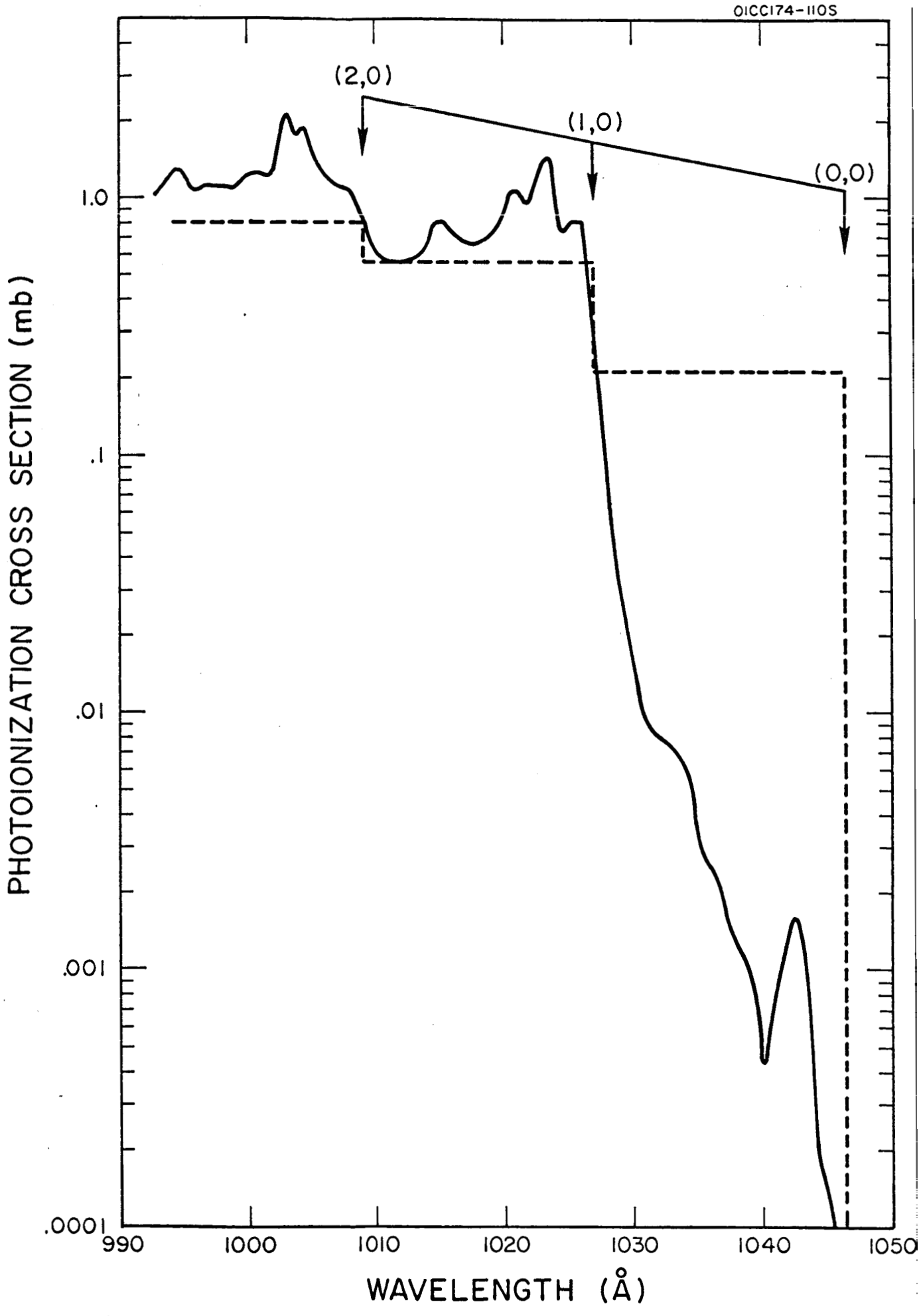

Figure 8. The photoionization cross section of O_2 as a function of wavelength. The dotted curve represents the theoretical cross section normalized to fit the experimental results in the (1,0) vibrational band.

ion current would be observed at low temperatures. To test this possibility, a special ion chamber was constructed which was suitable for decreasing the gas temperature (see Fig. 9). However, in the performance of subsequent runs, no change in the ion current was observed when the gas was cooled. Thus, it appears that the experimental evidence indicates that the observed ions cannot be due to the ionization of vibrationally-excited molecules. These negative results suggested the search for alternative sources of ion production such as:

(a) The possibility that O_4^+ was formed at high pressure due to the reaction

$$O_2 + h\nu \rightarrow O_2^* \quad ,$$

followed by:

$$O_2^* + O_2 \rightarrow O_4^+ + e$$

or

$$O_2^* + O_2 + O_2 \rightarrow O_4^+ + e + O_2.$$

For this process to be possible, the ionization potential of O_4 must be less than that of O_2. According to Curran,[29] who used electron impact techniques coupled with a mass spectrometer, the appearance potential of O_4^+ was 16.9 ± 0.1 eV; moreover, the pressure dependence of O_4^+ was cubic for pressures less than 0.2 torr. Curran proposed that the O_4^+ ions were formed by the three-body reaction

$$O_2^+ (a^4\Pi_u) + O_2 + O_2 \rightarrow O_4^+ + O_2 \quad ,$$

where the $a^4\Pi_u$ metastable state would necessarily be vibrationally excited. In the present work, the pressure dependence for ions formed at 1032Å was

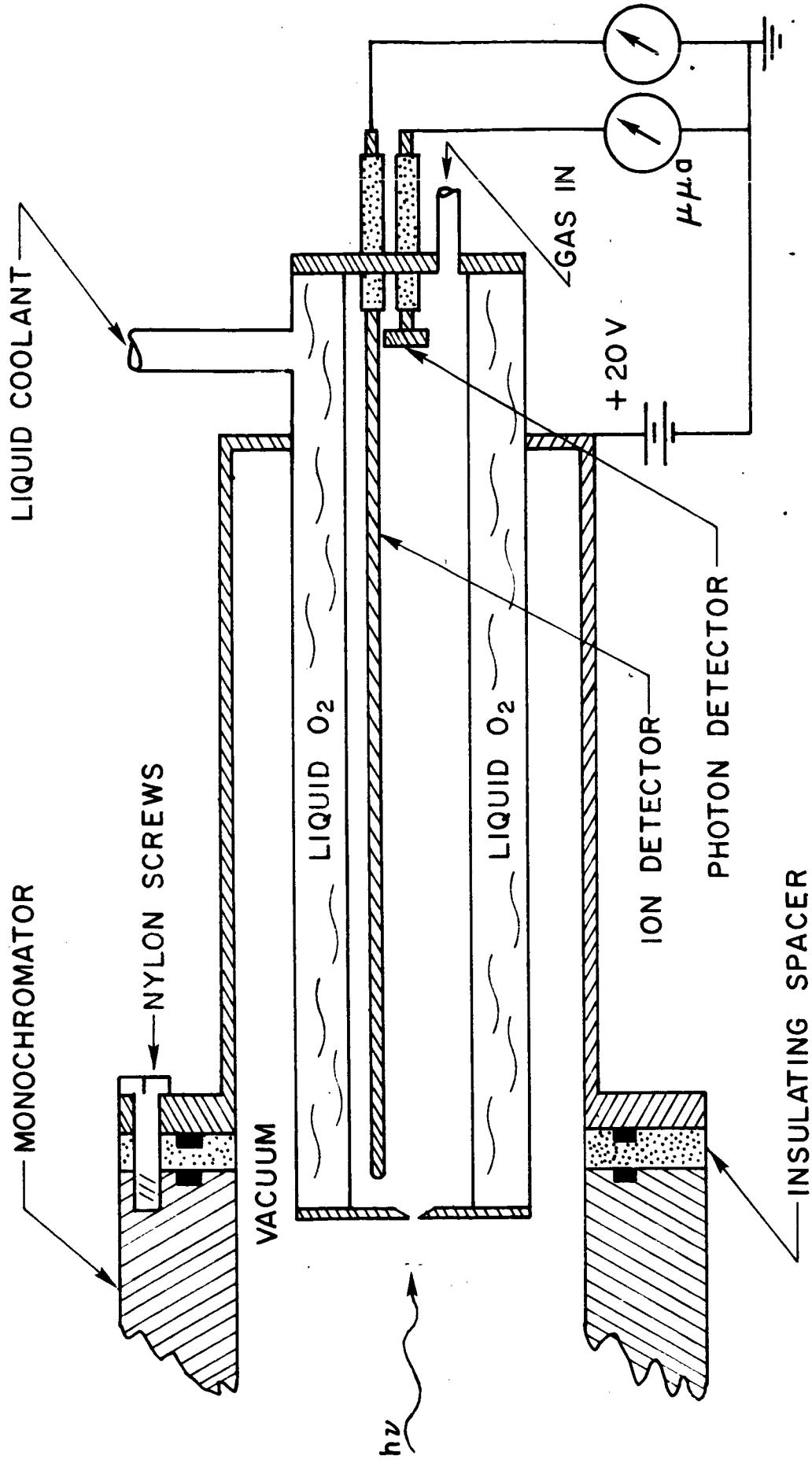

Figure 9. Ion chamber suitable for measurements at low temperature.

measured and found to be linear at low pressures, while at higher pressures it followed the law for direct ionization; namely, $i \propto [1 - \exp(ap)]$ where a is a constant and p is the pressure. Thus, the formation of O_4^+ at energies of 12 eV is not compatible with this observation of the work of Curran.

(b) It is possible for electrons to be released from the collector plate either by scattered radiation or by impacting O_2^* molecules. Such an effect would have the appearance of a positive ion current; however, the magnitude of the current would be dependent on the area of the collector plate. The rectangular collector plate (4 x 20 cm) was replaced by a thin wire; however, no change in the ion current was observed.

(c) The isotope effect. The natural abundance of O^{16} O^{18} is 0.2 percent. If the isotope had an ionization potential lower than O_2, this could account for the observed ions. However, since the electronic structure of isotopes is very similar, the differences in the ionization potentials are generally very small and in many cases, the shift is towards higher energies. In N_2, for example, the ionization potential of the isotope is increased by about 0.003Å.[30]

(d) Impurities: When no gas was present in the ion chamber, a residual ion current could be measured. The impurity ion current (probably due to oil vapor) had a definite appearance potential of 1278Å. Further, the new ion current increased linearly with pressure as discussed above. Zeolite traps were used to remove the residual ion currents and spectroscopically-pure oxygen was used in the ion source, but still the new ion current persisted.

(e) It is possible that the O_2^+ ions are formed by the process

$$O_2 + h\nu \rightarrow O_2^*$$

$$O_2^* + O_2 \rightarrow O_2^+ + O_2^- \quad .$$

The electron affinity of O_2 is given experimentally as 0.44 eV whereas the theoretical value is about 0.15 eV. At any rate, this process would lower the appearance potential of the O_2^+ ions by the magnitude of the electron affinity.

From (a), (b), (c) and (d) it would seem that the only conclusion that can be reached is that the ions are, in fact, O_2^+ ions. However, from (e) it is shown that O_2^+ may not be formed by direct photoionization. Experiments are being considered to differentiate between the direct process and the above postulated reaction.

C. PLANETARY AERONOMY

During the present Quarter, the effort under planetary aeronomy has produced significant results in two areas:

1. The photolysis of carbon dioxide in the Martian atmosphere
2. Measurement of the scattering cross section of xenon at Lyman-alpha.

1. The Photolysis of Carbon Dioxide in the Martian Atmosphere

The initial CO_2 photolyses studies performed under this program[31,32] consisted of a preliminary examination of the effects of solar ultraviolet radiation upon specific model Martian atmospheres that were based on a surface pressure of 85 mb and other then-accepted observational data. These results, obtained through desk calculations, were subsequently compared with results from a study programmed for a digital computer. Although these earlier studies used several simplifying approximations, such as an isothermal atmosphere and the neglect of successive iterations of the final number density distributions, they did provide a general insight into the problem by elucidating the formation of minor constituents and the general absorption characteristics of the model atmospheres employed.

Several current factors have combined to necessitate a reinvestigation of the original problem with much more thoroughness: (1) quantitative information on the chemical composition as a function of altitude is now required in the advent of planetary probes designed to penetrate the Martian atmosphere; (2) in recent years, theoretical studies of Mars have concentrated on vertical pressure and temperature profiles and although qualitative examinations of the atmospheric composition have been made, a rigorous study actually specifying limits for number densities apparently has not been conducted; (3) an unexpected revision of estimates regarding the relative abundances of atmospheric gases on Mars has very recently been made. The aim of the present study is to expand and update the preliminary work in view of these factors. Emphasis

is placed on the specific variation of composition with altitude rather than content or relative abundance, thus filling a gap in the current theoretical picture of the Martian atmosphere.

The detection of CO_2 absorption at 0.87μ by Kaplan et al.[33] and the subsequent analysis of 1.67μ absorption by Kuiper[34] have led to revised estimates for surface pressure and total content of the atmosphere of Mars. These data have important consequences both for the theoretical study of planetary atmospheres and for Mars probes. In particular, the revised surface pressure-value is considerably lower than previous estimates of about 85 mb (approximately 0.09 that of earth). In addition, the percentage of CO_2 in the atmosphere is significantly greater than earlier estimates. For the surface pressure, Kaplan et al. obtained a value of 25 ± 15 mb, while Kuiper's analysis gave 10 mb. According to Kaplan et al., the partial pressure of CO_2 is 4 ± 2 mb. If such is the case, CO_2 can no longer be considered only a minor constituent. Furthermore, through an analogy with the terrestrial argon abundance, Kaplan et al. suggest that argon with a partial pressure between 2 and 19 mb may also be a major atmospheric constituent on Mars.

Based on the results of the preliminary GCA studies, it was decided that the best approach to a complete investigation would be to construct a "grid" of various combinations of the surface pressures and total abundances suggested by the latest observational data. The photochemical number density profiles of a number of cases selected from this array,

representing all possible ranges, was then computed. An analysis of the results proceded along two directions. An average model was selected as representative of the most probable conditions. The general characteristics of the actual physical atmosphere are thus reflected in the discussion of a single case. Next, the effects of parameterization were obtained by a study of the departures in the other selected cases from the representative model.

It is very likely that observations will refine the experimental data on temperature, pressure and chemical content of the Martian atmosphere; however, it is not anticipated that subsequent data will be outside of the range of parametric values considered here. Thus, this study can provide a set of curves reflecting important atmospheric characteristics that will be valid for new observational data. Toward this end and within the limits of the "grid", functional relationships between those characteristics and the initial atmospheric parameters – specifically, temperature, surface pressure, CO_2 abundance and mean molecular weight – have been determined. The inclusion of mean molecular weight as a parameter obviates a specification of an argon: nitrogen ratio since both of these gases may be considered photochemically unreactive within the spectral region 900 to 3000Å. Their role in the reactions considered is restricted to that of a third body. Thus, the results should be valid even for the possible existence of other "filler" gases whose absorption properties do not allow an important photochemical role.

Many improvements have been added to the preliminary studies discussed in earlier reports, while significant restrictions have been removed.

The expanded problem is now solved by a three-part program on an IBM 1620 digital computer. In the first part, vertical number-density distributions of the initial atmospheric constituents are calculated. This program allows for a vertical temperature profile as well as a mictopause set arbitrarily at 200 km. The atmospheric temperature models by Schilling provided a surface temperature range of from 200 to 300°K, as determined from bolometric observations. The initial number densities together with recent solar flux data (900 to 3000Å) and absorption cross sections of the atmospheric gases serve as input data for the second sub-program which calculates the photodissociation rates so that the resulting constituent number-density altitude profiles could be calculated in the final part of the program. In the fully iterated solution, the output is fed back to the first sub-program and the process repeated. This iteration scheme is continued until convergence in the final distributions is obtained. The results of successive passes are not expected to be grossly different from the initial pass results as given here.

Some thirty-three "grid" cases were computed through the first pass. A tabulation of these results led to some significant and interesting conclusions. The format of each set of constituent number density-altitude curves for any one model was essentially the same. Particularly, the atomic and molecular oxygen distributions in semi-log coordinates are very nearly parabolic. It was evident from a comparison of the many curves that the distributions varied almost systematically according to initial parameters. The results can be displayed in an efficient and informative manner by showing

the altitudes of the peak particle densities of O and O_2 plotted as a function of mean molecular weight for several "partial pressures" of CO_2.

Figure 10 shows the first pass number density profiles for the representative case. Figure 11 shows the approximate altitude variation of the O and O_2 peak particle densities for P_o = 10 and 25 mb as a function of mean molecular weight. The CO_2 content was held constant at approximately 4 mb (2.5×10^{23} molecules/cm^2-column).

Two values of the total surface pressures, P_o, were investigated; namely, 10 and 25 mb. The results showed a consistently small difference — of the order of a few kilometers — between the P_o = 10 and P_o = 25 mb curves so that a mean value of 17 to 18 mb was chosen as a representative value for the surface pressure.

From a preliminary analysis of the data generated in this expanded study, it was possible to develop tentative empirical formulas permitting graphical construction of approximate number-density distributions for O and O_2. Thus, approximate model photochemical atmospheres can be conveniently simulated without the necessity of performing lengthy computer calculations as long as it is assumed that the distributions are functions of only mean molecular weight, surface pressure and total CO_2 abundance. The curves thus constructed from the empirical formulas are reasonably accurate within the following limits:

$$28 \leq \bar{m} \leq 44 \text{ (gms mole}^{-1}\text{)}$$

$$10 \leq P_o \leq 25 \text{ (mb)}$$

$$7.5\times10^{22} \leq N_{CO_2} \leq 2.25\times10^{23} \text{ (molecules/cm}^2\text{-column)}.$$

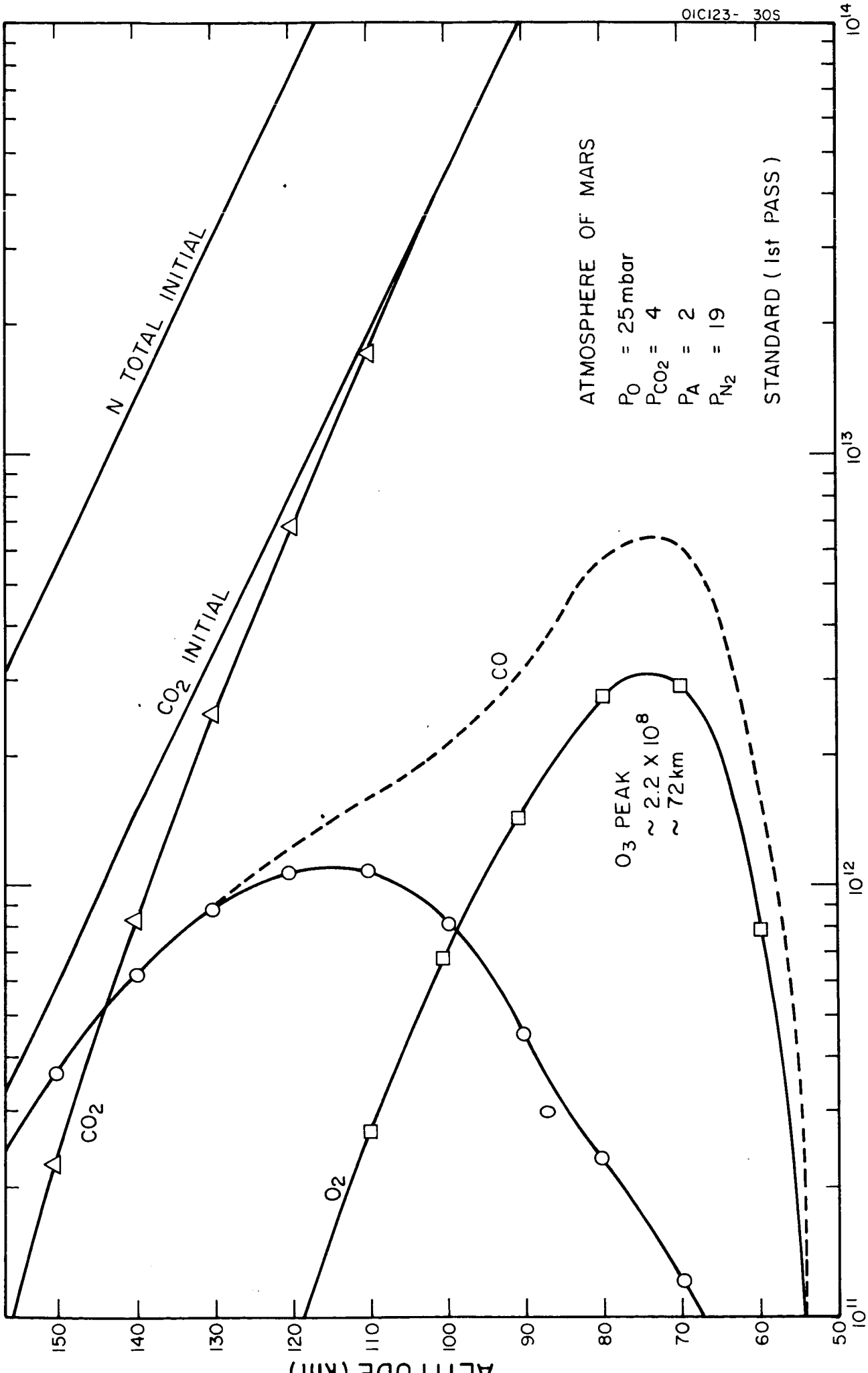

Figure 10. Altitude variation of particle density.

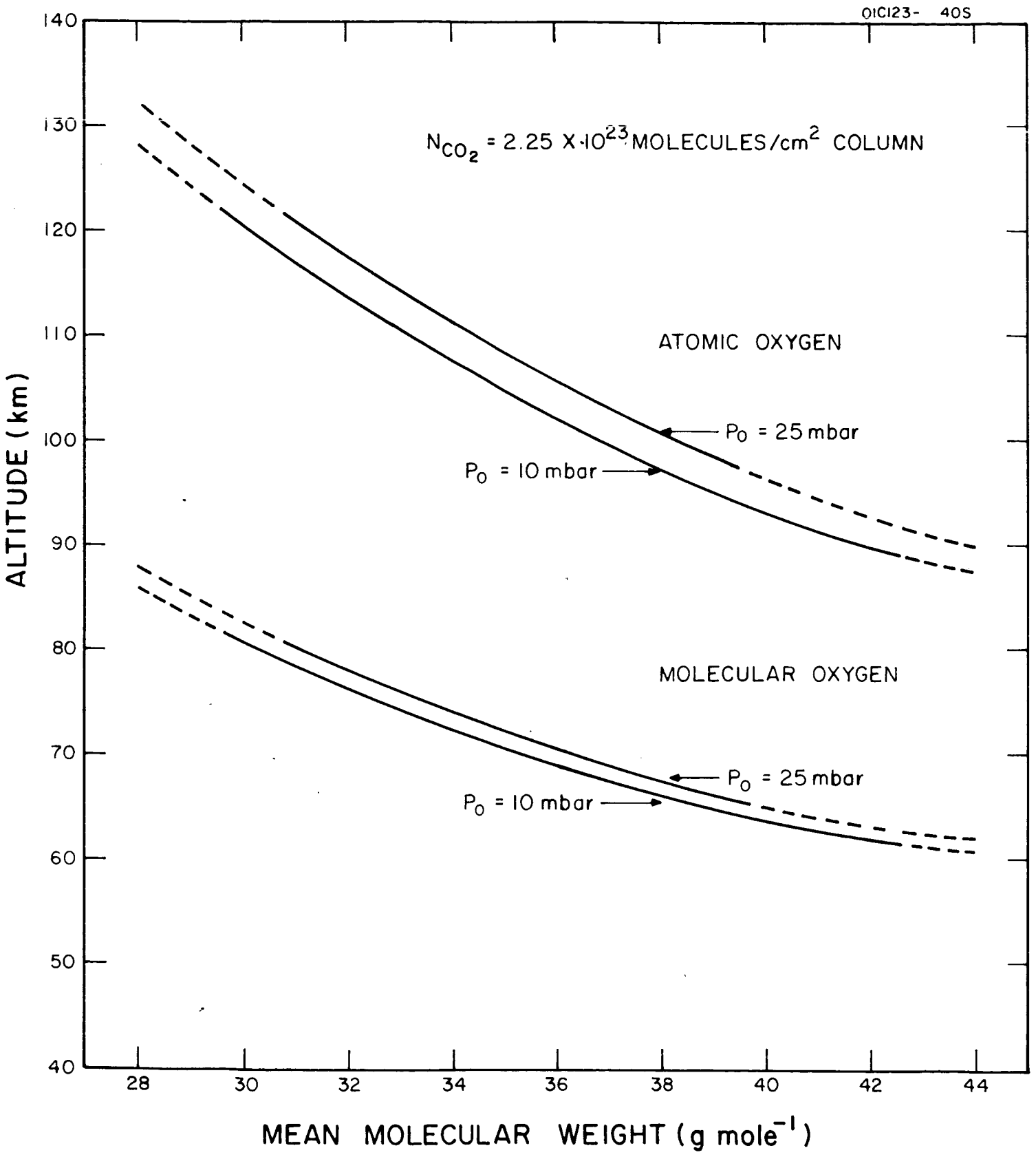

Figure 11. Variation of altitude of peak particle density for atomic and molecular oxygen with mean molecular weight and surface pressure.

The emphasis throughout the derivation of the tentative empirical formulas was placed on the distribution of atomic and molecular oxygen only. These profiles can be viewed as the major determining characteristics for the entire model photochemical atmosphere since the entire model may be constructed in the following fashion. The altitudes of the peak particle densities of O and O_2 are determined directly from the final composite curves. The values of the peaks are given by empirical formulas. From these data, the O and O_2 profiles are constructed by assuming parabolic distributions (semi-log coordinates), the semi-latus rectum of each being determined from a second set of empirical formulas. From these curves, the number densities of other photochemical constituents may be obtained. n(CO) is calculated from the mass balance equation

$$n(CO) = n(O) + 2n(O_2) + 3n(O_3) ,$$

where $n(O_3)$ may be neglected due to its secondary importance. $n(CO_2)$ is determined by the relation

$$n(CO_2) = n_I(CO_2) - n(CO) ,$$

where $n_I(CO_2)$ is the initial CO_2 particle density. The distributions of N_2 and A are unaffected by the photochemistry considered in this region of the atmosphere.

The positive results of the preliminary analysis and empirical formula derivations are encouraging. While a recomputation of the fully-iterated models and a refinement of the empirical formulas are appropriate

to a sophisticated and quantitative study, meaningfully different results are not anticipated in view of the necessary approximations included and the uncertainty of the initial parameters. Pending these refinements, there remain only the tasks of rechecking the distributions obtained from the empirical formulas against the computer results, preparing final presentations of the data, and writing an account of the efforts reflected by this study and the results.

2. Measurement of the Scattering Cross Section of Xenon at Lyman-Alpha

The relative cross sections at Lyman-alpha (1215.7Å) for A, Ne, He, H_2 and N_2 were previously measured by employing a microwave-powered hydrogen light source with an oxygen filter to isolate Lyman-alpha radiation. The resulting right-angle scattering was measured by a vacuum ultraviolet Geiger counter filled with nitric oxide. The scattering measurements have now been obtained for xenon and krypton and were found to disagree with the previously-reported measurements[35] by as much as one order of magnitude. As an additional experimental check and also in an attempt to change the relative cross-section values into absolute units, a new attenuation technique was devised. This technique employed a 2-meter grating vacuum monochromator, a hydrogen discharge light source, a 56 cm long attenuation cell made of Pyrex glass and a nitric oxide ion chamber as the detector. The experimental arrangement is shown in Fig. 12. Assayed reagent-type of xenon gas (5 parts per million nitrogen and no other detectable impurity) supplied by AIRCO in a one-liter Pyrex flask was used for the attenuation measurement.

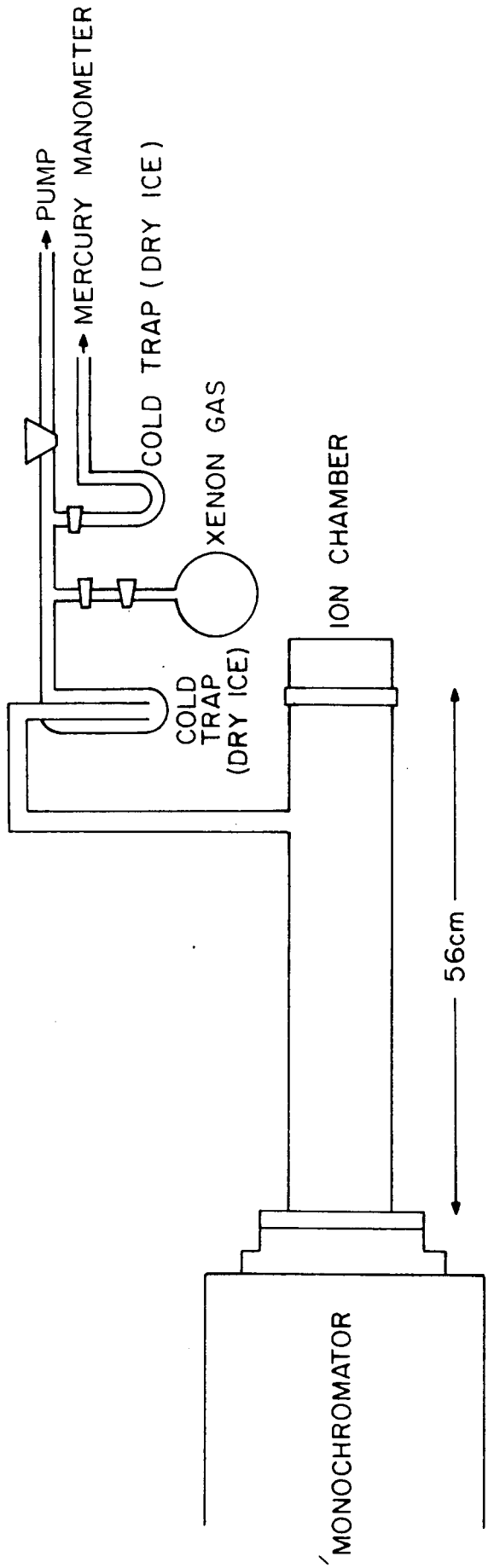

Figure 12. Experimental arrangement for attenuation of technique.

The attenuation of Lyman-alpha radiation was measured with increasing concentrations of xenon and then attenuation cross sections were calculated by the formula

$$\sigma = \frac{1}{nL} \ell n_e \frac{I_o}{I} \tag{17}$$

where

n = number density per cc

L = length of the attenuation cell

I_o = intensity of the incident light

and I = intensity of the attenuated light.

The calculated attenuation cross sections were plotted against the pressure of xenon and were not independent of pressure as expected by Eq. (17), but were found to increase linearly with increasing concentrations of xenon (see Fig. 13). These results could be explained as being due to the absorption of radiation by xenon molecules formed at higher pressures by the process $Xe + Xe \rightarrow Xe_2$. For example:

let n be the number density, so that

$$n = n\,(Xe) + n\,(Xe_2)\ .$$

Then if k is the equilibrium constant for the above reaction,

$$n\,(Xe_2) = kn^2(Xe) = kn_1^2$$

$$\therefore\ n = n_1 + kn_1^2$$

or

$$n_1 = \frac{1}{2k}\left[-1 \pm (1 + 4kn)^{\frac{1}{2}}\right].$$

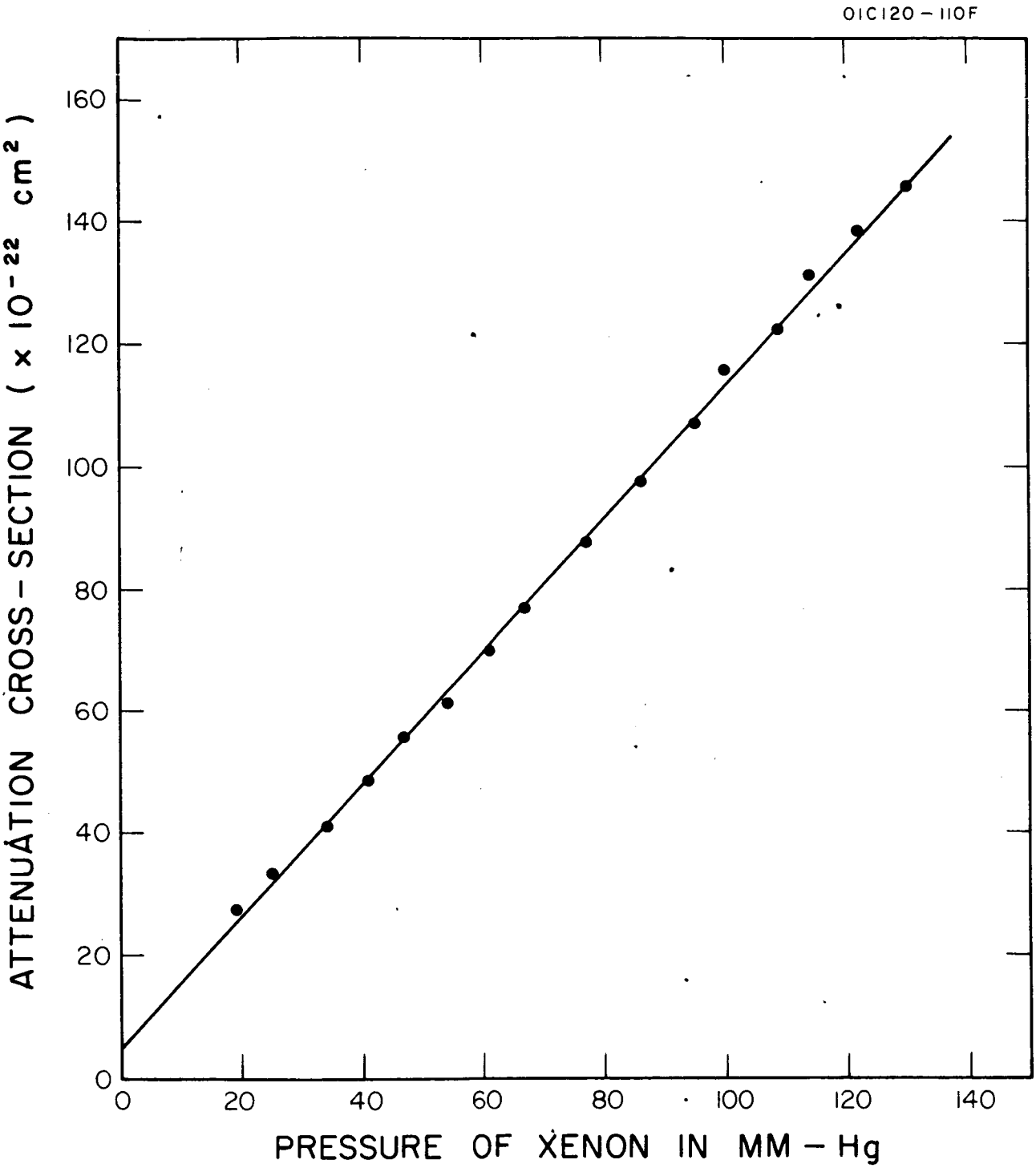

Figure 13. Variation of attenuation cross section with pressure.

Two cases have been considered. For Case I, let $1 > 4kn$; then expanding binomially,

$$n_1 = n.$$

The attenuation of light intensity in this case may be expressed as

$$I = I_o \exp\left[-\left(n_1\sigma_1 + kn_1^2\sigma_2\right) L\right] \tag{18}$$

where σ_1 is the scattering cross section for xenon atoms and σ_2 is the absorption cross section for xenon molecules. The above expression can be written as

$$\frac{1}{nL} \ell n_e \frac{I_o}{I} = \sigma_1 + k\sigma_2 n \qquad n = n_1$$

or

$$\sigma = \sigma_1 + k\sigma_2 n \quad . \tag{19}$$

For Case II, let $1 < 4kn$ such that $\sqrt{4kn} > 1$; then

$$n_1 = \sqrt{\frac{n}{k}} \quad .$$

In this case, the measured attenuation cross section is given by

$$\sigma = \sigma_2 + \frac{\sigma_1}{\sqrt{k}} \cdot \frac{1}{\sqrt{n}} \quad ; \tag{20}$$

i.e., σ varies inversely as $\sqrt{n}$.

It appears that Case I prevails and, therefore, the data can be explained by Eq. (17) where σ_1 is the intercept of the straight line on the Y-axis and $k\sigma_2$ is the slope. From Fig. 13, the value of the scattering cross section for xenon atoms, σ_1, is 5×10^{-22} cm^2; and the product of the equilibrium constant, k, and the absorption cross section, σ_2, for xenon molecules is 3×10^{-39} cm^5.

III. OTHER PERTINENT INFORMATION

During this Quarter, three meetings were attended by scientific personnel involved in this program.

Dr. F. F. Marmo attended the AGU Meeting held in Washington, D. C., on April 19, 1965. Several stimulating papers were given which were directly related to the scientific content of this program. In many cases, it was found that these latest scientific findings could be integrated into the current program so that duplication of effort could be minimized.

Dr. J.A.R. Samson presented an invited paper entitled "Photoionization Processes" at the Thirteenth Annual Conference on Mass Spectroscopy and Allied Topics held in St. Louis, Missouri, on May 17-18, 1965. The paper was warmly received and also the subject of some stimulating discussions. In addition, several other papers were presented on the subject of the photoionization of gases. Many of these involved the coupling of a mass spectrometer with a vacuum monochromator. Fruitful discussions on electron energy measurements were held with Dr. Schoen from the Boeing Scientific Laboratories.

Dr. J.A.R. Samson presented an invited paper entitled "Oscillator Strengths in the Noble Gases" at the Thirteenth Annual Meeting of the Radiation Research Society held in Philadelphia, Pa., on May 25-26, 1965. Dr. Y. Tanaka discussed light sources in which he demonstrated the need for further effort in this area. Dr. McNesbie spoke on photochemistry whereas Dr. Person discussed photoionization, excitation and dissociation in molecular gases. These topics are directly related to the current research program.

REFERENCES

1. GCA Technical Report No. 65-16-N, Final Report, Contract No. NASw-840, April 1965.

2. Cuthbertson, C. and M. Cuthbertson, Proc. Roy. Soc. A135, 40 (1932).

3. Dalgarno, A. and A. E. Kingston, Proc. Roy. Soc. A259, 424 (1960).

4. Karplus, M., J. Chem. Phys. 37, 2773 (1962).

5. Karplus, M. and H. F. Kolker, J. Chem. Phys. 39, 1493, 2997 (1963).

6. Yaris, R., J. Chem. Phys. 39, 2474 (1963).

7. Yaris, R., J. Chem. Phys. 40, 667 (1964).

8. Levine, H. B. and H. S. Taylor, J. Chem. Phys. 41, 1367 (1964).

9. Dalgarno, A., Quantum Theory, Vol. 1, ed. D. R. Bates (Academic Press, New York, 1961).

10. Dalgarno, A., Rev. Mod. Phys. 35, 522 (1963).

11. Hart, A. and G. Herzberg, Phys. Rev. 106, 79 (1957).

12. Schwartz, C., Phys. Rev. 123, 1700 (1961).

13. Dalgarno, A., R. J. W. Henry and A. Stewart, The Photoionization of Atomic Oxygen, Planetary Space Sci. 12, 235 (1964); GCA TR 64-1-N (January 1964).

14. Huffman, R. E., Y. Tanaka and J. C. Larrabee, Disc. Faraday Soc. 37, 159 (1964).

15. Cook, G. R., B. K. Ching and R. A. Becker, Disc. Faraday Soc. 37, 149 (1964).

16. Samson, J. A. R. and R. B. Cairns, J. Geophys. Res. 69, 4583 (1964).

17. Schoen, R. I., J. Chem. Phys. 40, 1830 (1964).

18. Aboud, A. A., J. P. Curtis, R. Mercure and W. A. Rense, J. Opt. Soc. Am. 45, 767 (1955).

19. Weissler, G. L. and Po Lee, J. Opt. Soc. Am. 42, 200 (1952).

20. Po Lee, J. Opt. Soc. Am. 45, 703 (1955).

21. de Reilhac, L. and N. Damany-Astoin, C. R. Acad. Sci. Paris 258, 519 (1964).

22. Weissler, G. L., Po Lee, and E. I. Mohr, J. Opt. Soc. Am. 42, 84 (1952).

23. Curtis, J. P., Phys. Rev. 94, 908 (1954).

24. Vodar, B., J. Quant. Spectroy. Radiative Transfer 2, 393 (1962).

25. Quarterly Progress Report No. 4, Contract No. NASw-840, October 1964.

26. Inn, E. C. Y., Phys. Rev. 91, 1194 (1953).

27. Watanabe, K. and F. F. Marmo, J. Chem. Phys. 25, 965 (1956).

28. Nicholson, A. J. C., J. Chem. Phys. 39, 954 (1963).

29. Curran, R. K., J. Chem. Phys. 38, 2974 (1963).

30. Ogawa, M., Can. J. Phys. 42, 1087 (1964).

31. Marmo, F. F. and P. Warneck, NASA Contract NASw-124,GCA Tech. Rpt. 61-20-N (1961).

32. Marmo, F. F., P. Warneck, A. C. Holland and E. D. Schultz, GCA Quarterly Progress Rpt., Contract NASw-395, Nov. (1962).

33. Kaplan, L. D., G. Münch and H. Spinrad, Astrophys. J. 139 1 (1964).

34. Kuiper, G. P., Fifth Semiann. Status Rpt. to NASA Lunar and Planet. Lab., U. Arizona Res. Grant NsG 161-61, Dec. (1963).

35. Gill, P. and D. W. O. Heddle, J. Opt. Soc. Am. 53, 847-851 (1963).